Methods for vibro-acoustic diagnostics of turbine cavitation

Méthodes pour le diagnostic vibro-acoustique de la cavitation de turbine

BRANKO BAJIC, *Korto Cavitation Services; Korto GmbH; 12, rue Ste Zithe; L-2763 Luxembourg; korto@cavitation.de; www.cavitation.de*

ABSTRACT
Basic aspects of noise sampling, signal processing and analysis, and data processing, analysis, and interpretation in vibro-acoustic diagnostics of turbine cavitation are investigated in a series of prototype and model experiments. Several weak points of the practice are identified, and improvements and new techniques are developed. These techniques enable extraction of data on cavitation details and early detection of detrimental effects met in turbine exploitation. A brief review of weak points of the practice, developed improvements, and new techniques, as well as examples of application, are presented in the paper.

RÉSUMÉ
Des aspects de base de l'enregistrement du bruit, des traitements et analyses analogiques et numériques des signaux, avec leur interprétation dans le diagnostic vibro-acoustique de la cavitation de turbine, sont étudiés dans une série d'expériences de prototype et de modèle. Plusieurs points faibles de la pratique sont identifiés, et des améliorations et de nouvelles techniques sont développées. Ces techniques permettent l'extraction de données sur des détails de cavitation et la détection précoce des effets néfastes rencontrés dans l'exploitation de turbine. Un bref examen des points faibles de la pratique, des améliorations développées, et de nouvelles techniques, aussi bien que des exemples d'application, sont présentés dans le papier.

Introduction

The art of vibro-acoustic diagnosis of erosive cavitation in hydro turbines has matured sufficiently to produce reliable practical results. The current state of knowledge in this discipline is well described by Bourdon et al. [1] in their report on the strong correlation between the vibro-acoustic signature of cavitation and the intensity of cavitation erosion, and by Farhat et al. [2] who report direct evidence that cavitation aggressiveness can be measured via a non-rotating vibro-acoustic sensor placed in a convenient location on a turbine.

Although vibro-acoustic methods for cavitation diagnostics thus have a firm foundation, the methods are still undergoing intensive research [1-19]. One line of this research is concerned with methods of sampling the vibro-acoustic field of cavitation in a turbine; processing and analysing sampled signals; and processing, analysing, and interpreting data derived from them. A series of experiments performed by the author on prototypes and models of Kaplan, Francis, and bulb turbines revealed some weak points in commonly used procedures, and resulted in improvements as well as in development of several new techniques [7,10,16,19], which were successfully verified in practical use [15,17,18]. A brief review of this development and some examples of applications are given here.

Tasks

When devising methods for noise sampling, processing and analysis, and methods for data processing, analysis, and interpretation, the following explicit or implicit tasks of vibro-acoustic diagnostic tests of hydro turbine cavitation have to be considered:

1. Extract cavitation-related signal components from the mixture of flow noise, machinery noise, and other disturbances.
2. Suppress cavitation-irrelevant effects induced by vibro-acoustic characteristics of machinery.
3. Identify different cavitation mechanisms and recognise the erosive ones among them.
4. Extract necessary data on the erosive mechanisms, and estimate the dependence of the erosion rate on turbine operational conditions.
5. Reveal the role various turbine parts play in the cavitation process.
6. Predict cavitation characteristics of a turbine after uprating or refurbishment.
7. Devise a rationale for a cavitation monitoring system selective with respect to turbine parts.
8. Ensure, in cavitation monitoring, high enough sensitivity to early detrimental effects.

From sampling to interpreting

Noise level as a cavitation estimator. The simplest and most often used vibro-acoustic estimator – cavitation noise level in a fixed frequency band – yields a biased estimate of cavitation intensity. A case showing this is illustrated in Fig. 1. If cavitation intensity were estimated by the noise level within any limited frequency band, the estimates of the ratio of intensities of the two cavitation mechanisms, having very differing spectra, would heavily depend on the choice of the frequency band. Because the true ratio of the mechanisms' intensities is fixed, such an estimator is hardly applicable. Further, there is no frequency band in which both mechanisms produce strong noise, thus there is no band within which they both can be assessed reliably. This implies that total power

Revision received June 28, 2002. Open for discussion till June 30, 2003.

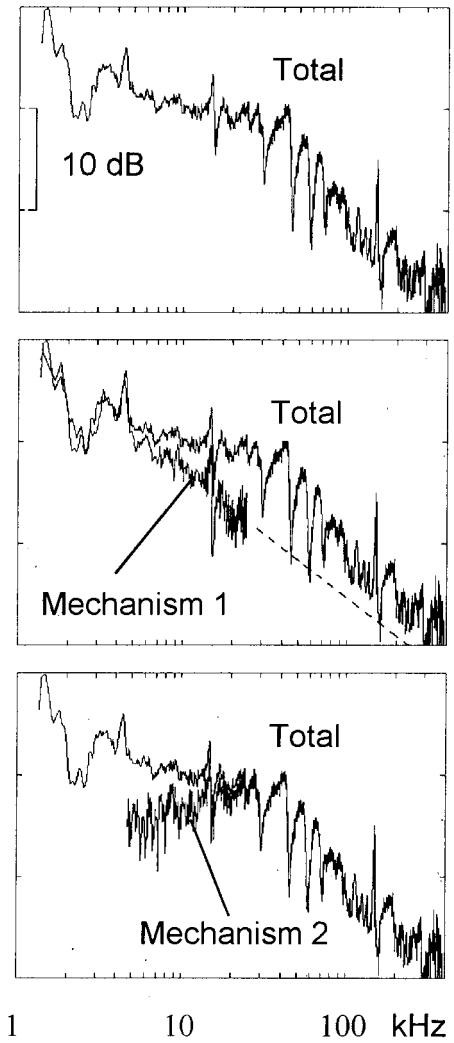

Fig. 1 Noise sensed in a cavitating turbine decomposed into two components generated by two distinct cavitation mechanisms. The mechanisms are found to be independent, thus noise power components are additive. The mechanisms' spectra are very different and have very little overlap.

and total spectrum of vibro-acoustic signals should be used instead of noise level in a limited frequency band.

Blade-passage-frequency modulation level was proposed by Abbot [3] as a measure of erosion aggressiveness of turbine cavitation. Some authors and institutions use that quantity as a universally valid estimator. However, there are reports on cases where there was significant erosion but the blade-passage-frequency modulation level was negligible [7,20].

Single-sensor estimates, i.e., estimates derived by means of a sensor in only one position, are biased. Both the mean noise power (Fig 2) and the short-time averaged noise power describing the influence of the runner angular position (Fig. 3) are found to depend strongly on the angular position of a sensor. In order to get noise descriptions which would be representative of all the parts of cavitation flow, a kind of spatial averaging is necessary. A result of such a processing is illustrated in Fig. 4.

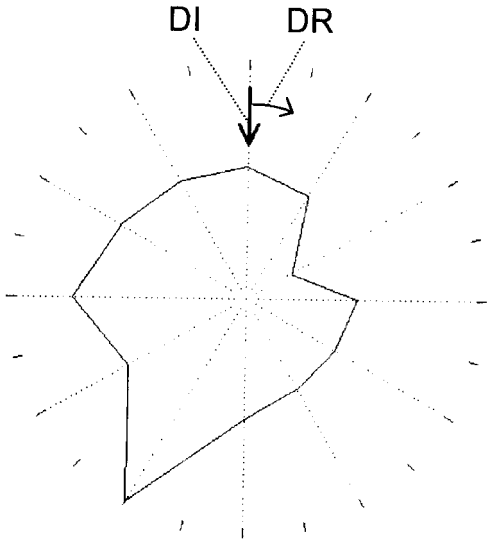

Fig. 2 Vibro-acoustic sensors placed in 12 locations around the runner of a cavitating Kaplan turbine resulted in the shown nonuniform circumferential distribution of the mean noise power. DI – direction of inflow into the spiral, DR – direction of rotation.

Circumferentially averaged noise signature can deliver representative estimates of erosion intensity only for highly developed cavitation. In most practical cases, analyses resolving the runner's angular position are necessary (Fig. 3 and 4).

Spectral format of modulation analysis results, used by some authors to assess turbine cavitation [2], ignores an important portion of the information, due to inherent circumferential averaging. The modulation waveform, expressed in the angular variable specifying the runner's position, must also be considered. This is espe-

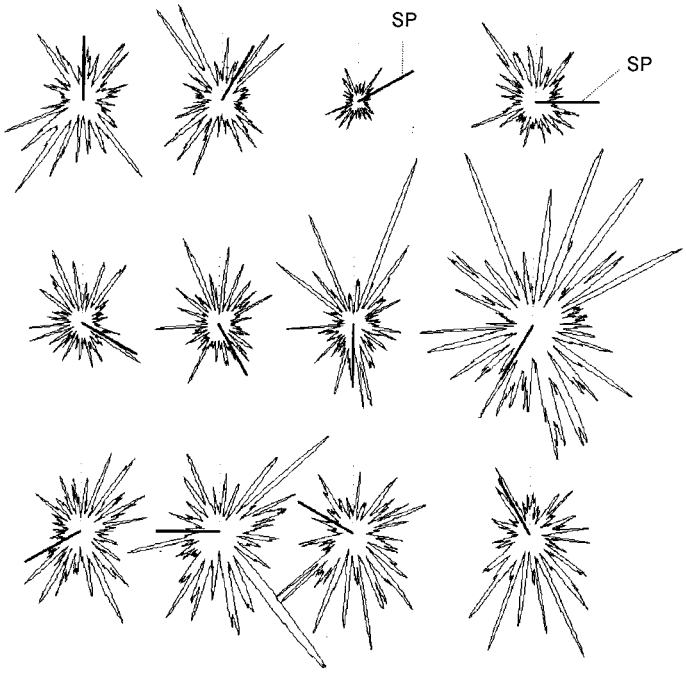

Fig. 3 Analysis of the noise power dependence on the angular position of the runner, performed by means of the sensors in 12 circumferential positions, yielded strongly differing modulation patterns. SP – sensor angular position.

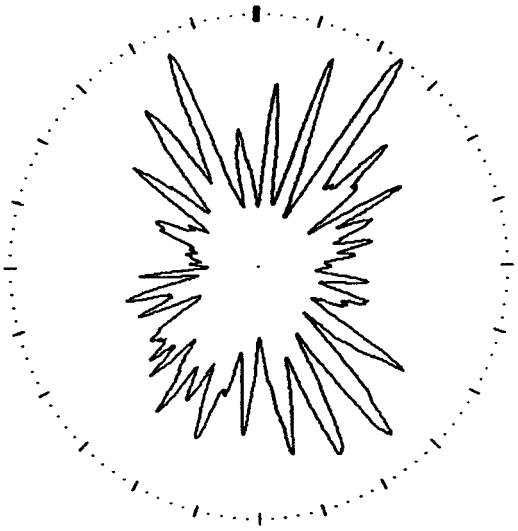

Fig. 4 Results from a 'synthetic' sensor: noise power sensed in 12 points around the runner averaged over these points.

cially important in applications aiming at an early detection of detrimental effects, which can hardly be expected to be uniformly distributed over the runner.

Low-frequency sensors, i.e., the ones functioning only below 0.1 MHz; resonant sensors used as such (attractive due to their high sensitivity); sensors used as non-resonant but having strongly pronounced resonances; sensors mounted in a way which enhances non-direct wave propagation from important cavitation regions to the sensor; and sensors mounted in a way which makes a part of a turbine casing or a guide-vane blade function as a collector of vibro-acoustic energy have been used in vibro-acoustic diagnostics of turbine cavitation. All of these sensors have the following disadvantages: *(i)* they do not enable high enough angular resolution (Fig. 5) needed to distinguish between pulses of modulation curves like those in Fig. 3; *(ii)* they often yield a lower signal-to-noise (cavitation-to-non-cavitation) ratio than the sensors operating at higher frequencies; and *(iii)* in most cases they ignore an important portion of noise energy, while the total noise power is needed for a non-biased estimate of cavitation intensity. Therefore, broadband high-frequency sensors should be used, and their location and way of mounting on the turbine have to be optimised for the type of analysis planned.

Several cavitation mechanisms are often co-existing in a turbine, either simultaneously or in different operational conditions. In such cases, the dependencies on turbine operational conditions, if derived from circumferentially averaged data, are physically meaningless. Thus, they should be studied separately for each component and then synthesised to yield an estimate of the total effect. The substantial differences in angular distribution of noise power generated by distinct mechanisms are shown in Fig. 6. Here, differences in spectra of the mechanisms (see Fig. 1) enabled attribution of the modulation curves as noted.

Different turbine parts can be involved in different forms of cavitation, which may have different circumferential dependencies. Thus, analyses aiming at identification of the contributions of different turbine parts to cavitation must not involve circumferential averaging of raw data. Instead, components related to different parts have to be estimated first, and only then may further processing be performed.

Novel techniques

Spectrum normalisation technique is based on the fact that transfer functions describing vibro-acoustic characteristics of a turbine do not depend on cavitation. Thus, if a noise power spectrum density, $G(f,P)$, measured at a turbine power P, is compared to the spectrum measured at a suitably chosen reference power, P_0, the two spectra will share effects due to turbine's and sensor's vibro-acoustic characteristics, so that their ratio – normalised spectrum,

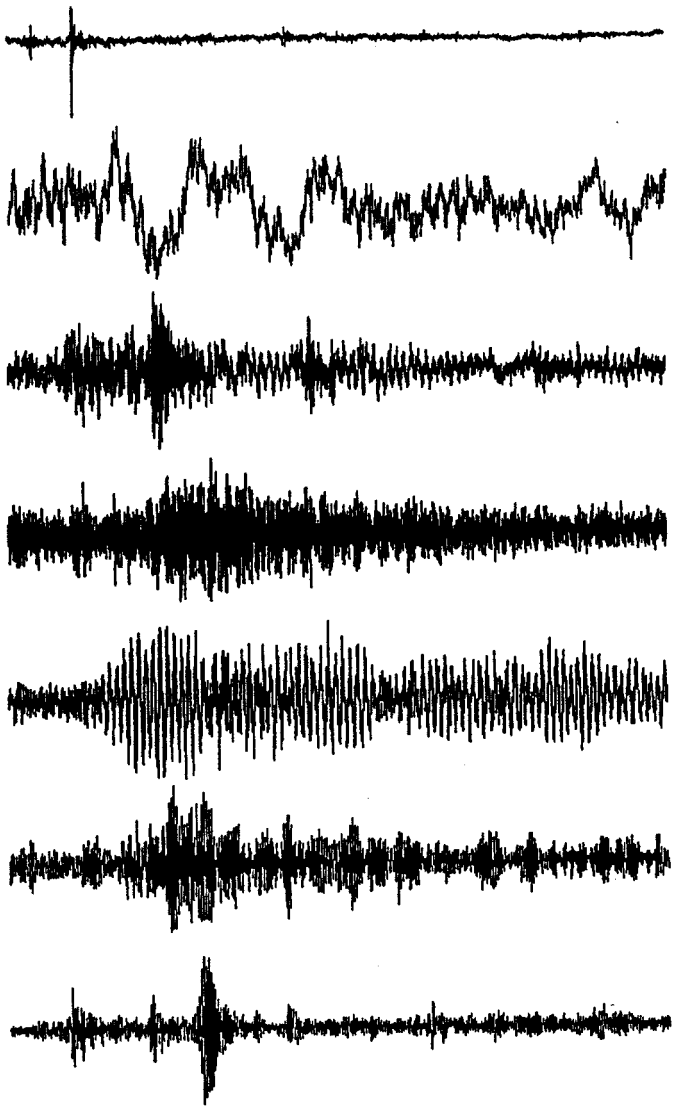

Fig. 5 Ten millisecond time samples of responses to an isolated cavitation pulse, obtained by four types of vibro-acoustic sensors mounted in several locations on a turbine. While the first waveform – obtained by a fast pressure transducer flush mounted in the turbine casing at the pressure side – shows primarily the undistorted direct wave, the others are more resonant and thus blur time and angle dependencies.

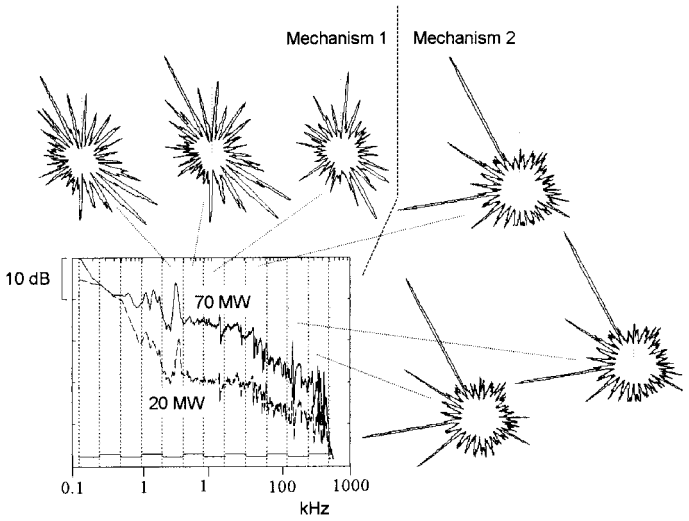

Fig. 6 The frequency-resolved analysis of the kind presented in Fig. 3, applied to the (total) signal considered in Fig. 1 (70 MW), revealed strong differences between the two mechanisms functioning in the turbine. 20 MW lies below the cavitation threshold.

$\gamma(f,P)=G(f,P)/G(f,P_0)$ – will suppress these cavitation-irrelevant data and yield a pure estimate of the dependence of cavitation intensity on P. This makes different sensors equally applicable and broadens their working frequency range (Fig. 7). However, these useful consequences of the spectrum normalisation concern only mean spectra, not necessarily the angular resolution (i.e., the effects illustrated in Fig. 5).

Inflow decomposition technique enables extraction of data on cavitation mechanisms from modulation curves like those shown in Figs. 3, 4, and 6. An example of such decomposition is presented in Fig. 8. Here, one of the high-frequency curves of Fig. 6, related to the mechanism 2, is drawn as Fig. 8a over the nets of angular positions denoting the interaction of the runner blades and the guide vanes. Two blades out of a total of five are considered, blade 4 and blade 5, and for each of them the traces of all the 24 guide vanes are drawn. The coincidence of a pulse of the modulation curve with the position of a particular blade/vane-pair shows that the flow disturbance induced by that pair is responsible for the generation of the pulse. The resulting decomposition of the total modulation curve is presented in Fig. 8b. The two blades were sufficient to exhaust the original curve. The conclusion follows: Blade 4 cavitates rather weakly in its interaction with all the vanes, strong however only behind guide vanes 16 and 18. Blade 5 cavitates significantly only behind guide vanes 16 and 18. Thus, of 5 runner blades and 24 guide vanes, only two runner blades in interaction with only two guide vanes are cavitating. Because the other three runner blades and the other 22 guide vanes produce no problems, they can serve as a reference in the repair.

Crest-factor distribution describing the pulse character of cavitation noise enables distinguishing between cavitation noise and background noise as well as distinguishing between cavitation mechanisms (Fig. 9).

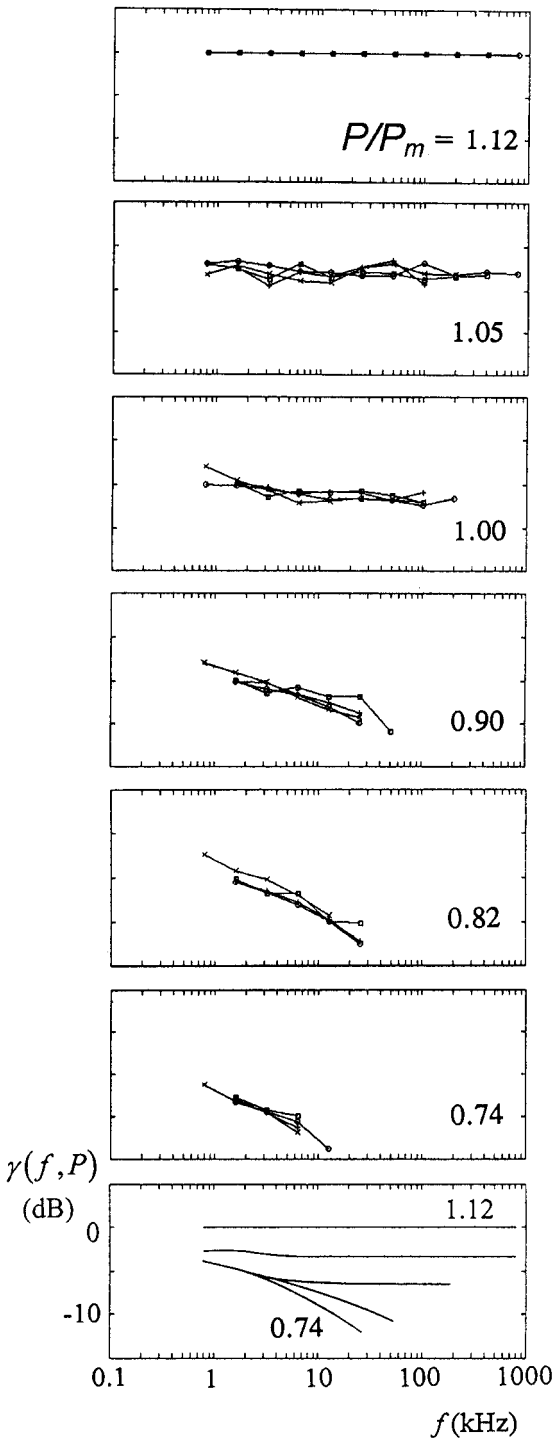

Fig. 7 Normalised spectra derived by means of four different types of sensors yielded estimates as sketched in the figure at bottom (P_m is the full turbine power). The individual estimates differ from these by only a few decibels.

Reliable background estimates can be obtained by relying on the pulse character of cavitation noise. Indeed, if, in operational condition in which there is cavitation, only noise samples in which no pulses appear are included in the spectral estimate, then an estimate of the background noise will be obtained. Such an estimate, derived directly in the condition considered, is more realistic than the estimate derived by extrapolating data from subcritical operational conditions.

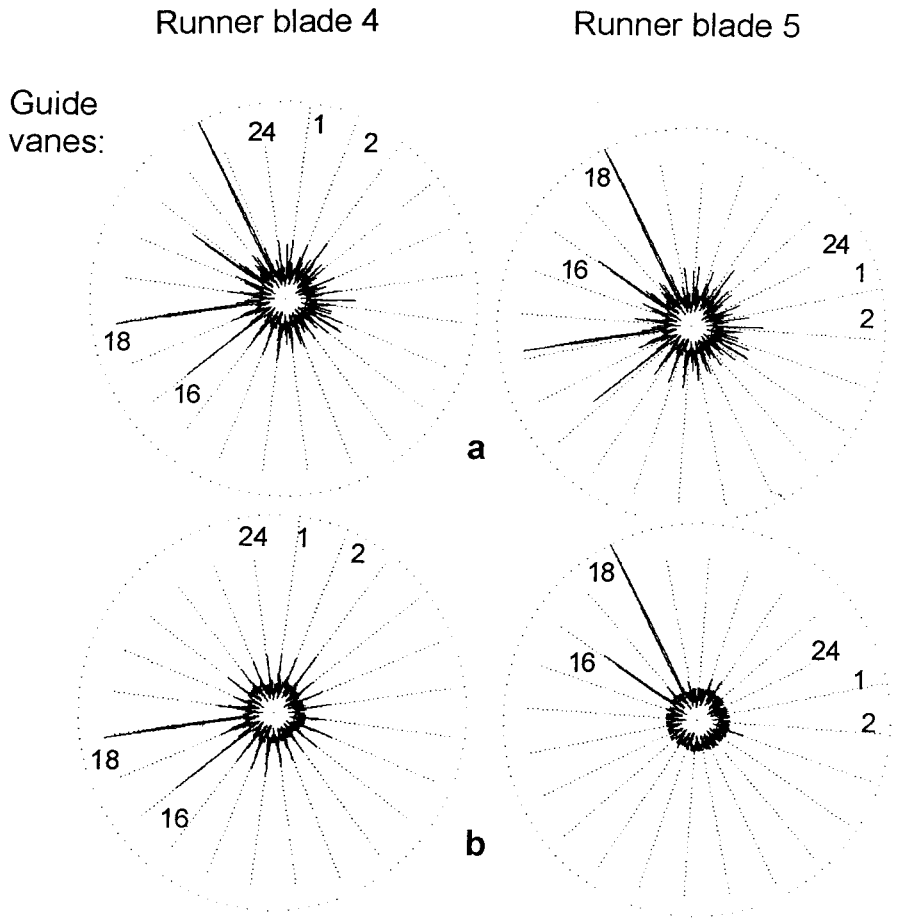

Fig. 8 Interpretation of the modulation curves of the mechanism 2 (Fig. 6): a – original curve, b – components describing the contributions of the two runner blades. Diagnostic result: Only two of five runner blades and only two of 24 guide vanes are responsible for cavitation.

Peak-selective spectrum, derived as a normal spectrum but from noise samples which contain only pulses higher or lower than a chosen limit, enables the described way of estimating the background and is also useful with respect to cavitation as well. Two such spectra, $\hat{\gamma}(f,P)$, are shown in the left column of Fig. 10. In one of them only the samples with peaks belonging to the highest 5% of all the peaks are taken into account, and in the other one only the samples with the lowest 5% of the peaks. While the latter estimates the background, the former is due to pure cavitation. The comparison of the two spectra in a series related to various turbine power values furnishes the diagnosis: A – no cavitation, B – mechanism 1 as above, C – mechanism 2.

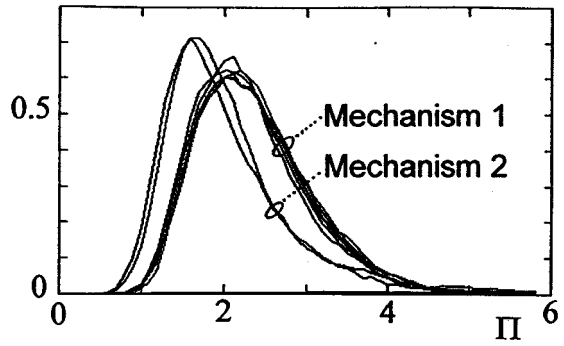

Fig. 9 Probability density function of the crest-factor, Π, estimated at several turbine power values, distinguishes between the two mechanisms of Fig. 1 and 6.

Spectral crest-factor, shown as $F_s(f,P)$ in Fig. 10, was derived from the same signals as $\hat{\gamma}(f,P)$ shown there. By generalising the crest-factor, which is the ratio of the peak and root-mean-square value of a signal, $F_s(f,P)$ is defined as the ratio of the $\hat{\gamma}(f,P)$ derived from the highest peaks and the normal mean spectrum, both being defined as power spectra. As can be seen, both spectral descriptions, peak-selective spectra directly and such spectra in a normalised form – as the spectral crest-factor, yield similar, quite interpretable and useful data.

Spectrum tracing is another technique for identification of cavitation mechanisms. In this technique one looks, under different operational conditions of a turbine, for similarities in the form of the mean spectrum and the form of weak variations in spectra which are rapidly varying in frequency. The latter can be shown to convey differences in transfer functions, so that a similarity found in a frequency range and bands of parameters describing operational condition points to a common location of the noise source, thus of a cavitation mechanism, too. By such an analysis in the noise-frequency/cavitation-number plane, four different mechanisms were identified on a model of a Francis turbine, where the experi-

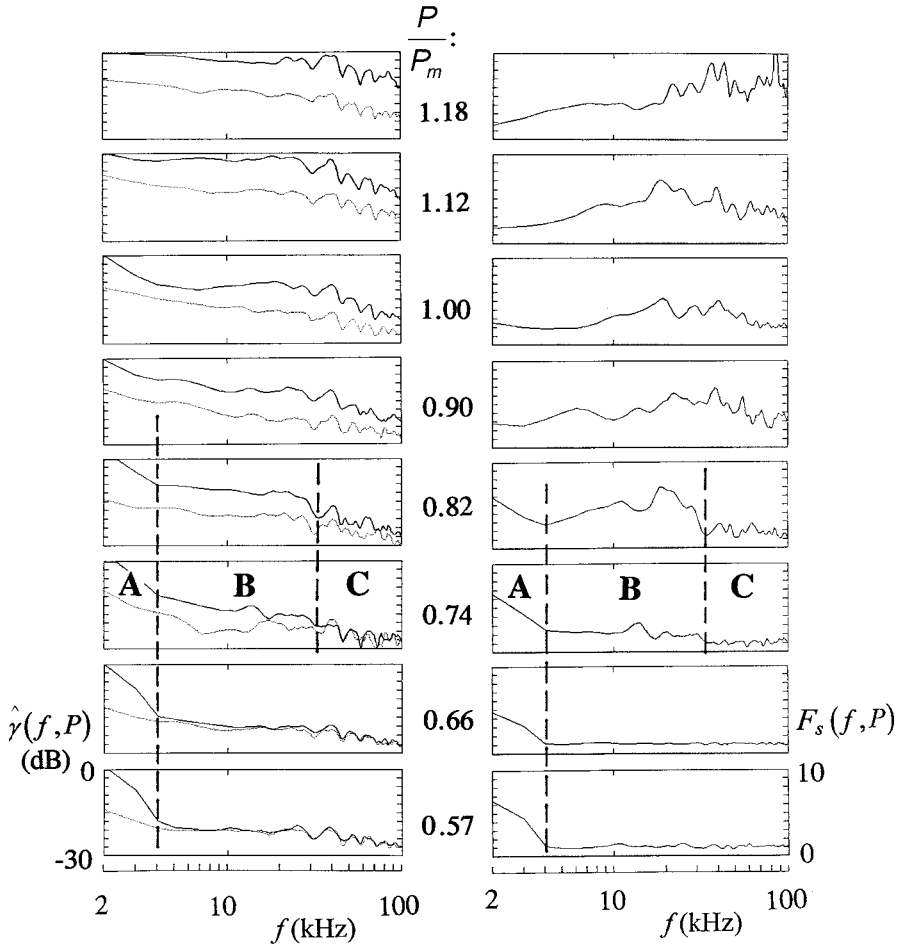

Fig. 10 Peak-selective spectra (left) and spectral crest-factor (right) derived from the same signals, sensed at the power *P*. B and C are identified as the mechanisms 1 and 2 described in Fig. 1, 6, and 9.

ment presented in Fig. 11 was made. The figure presents the continuation of the diagnostic procedure – the identification of spectral components. Here, for three (C, D, and E) of the identified mechanisms (B, C, D, E), spectra are estimated. Using further data obtained in the model test, the following conclusion was reached in this case: C is due to the hub-vortex cavitation, D the leading-edge cavitation, and E the trailing-edge cavitation. The difference in spectra enabled estimation and then also rejection of the erosion-irrelevant hub-vortex cavitation. Also, the leading-edge cavitation, which could not be seen due to the inconvenient form of the runner, was successfully assessed by vibro-acoustic means.

Empirical modelling. By tracing noise spectra as they depend on the operational parameters of a turbine, one can distinguish between contributions stemming from distinct cavitation mechanisms and assess their spectra. In this way one makes a decomposition of the measured spectra. Here, components of noise power generated by distinct mechanisms can be considered additive.
Several means can be used to recognise the components and estimate their spectra. The interpretation noted in Fig. 1, for example, was obtained by comparing the forms of low-frequency portions of the spectra at a series of power values, and by doing the same with the high-frequency portions. This showed the coincidence of groups of spectra within certain power- and frequency-intervals. Therefore, the forms of spectra of the mechanisms, their power-dependence, and the power intervals in which they function, were determined.
The mechanisms can also be recognised by means of modulation curves (Fig. 6), distribution of noise peaks (Fig. 9), more complicated spectral descriptions (Fig. 10), or non-systematically, by pure empirical reasoning (straight lines in Fig. 11 describing the mechanism E). Quite often, an empirical approach yields rather reliable fully quantitative data. Such an example is presented in Fig. 12. Here, noise power, $I(P)$, at the turbine power P, used as an estimate of the cavitation intensity, could be simply modelled by the exponential rule:

$$I(P) = \sum_{m=1}^{M} I_m(P)$$

$$I_m(P) = I_m\left[1 - \exp\left((P - P_c^m)/P_s^m\right)\right], \quad P > P_c^m,$$

$$I_m(P) = 0, \qquad P < P_c^m.$$

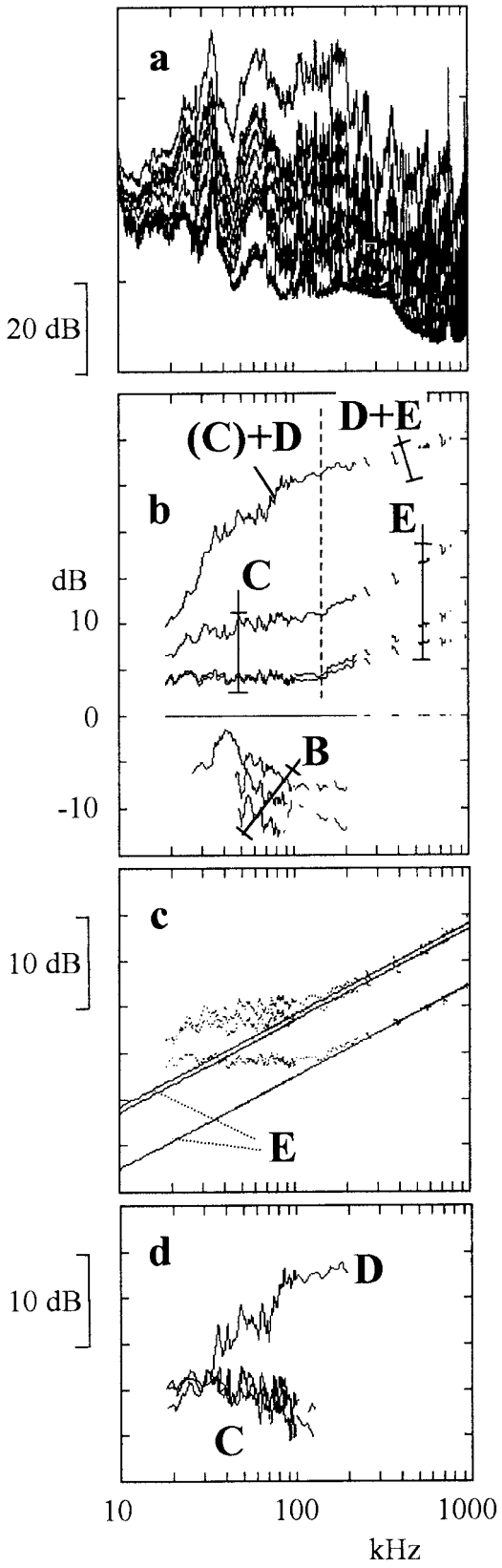

Fig. 11 Spectrum decomposition: a – raw spectra measured at several values of the cavitation number; b – these spectra normalised by the threshold spectrum, background subtracted; c – recognition of a high-frequency component (mechanism E); d – estimation of the form of the spectra of C=Total-E and D.

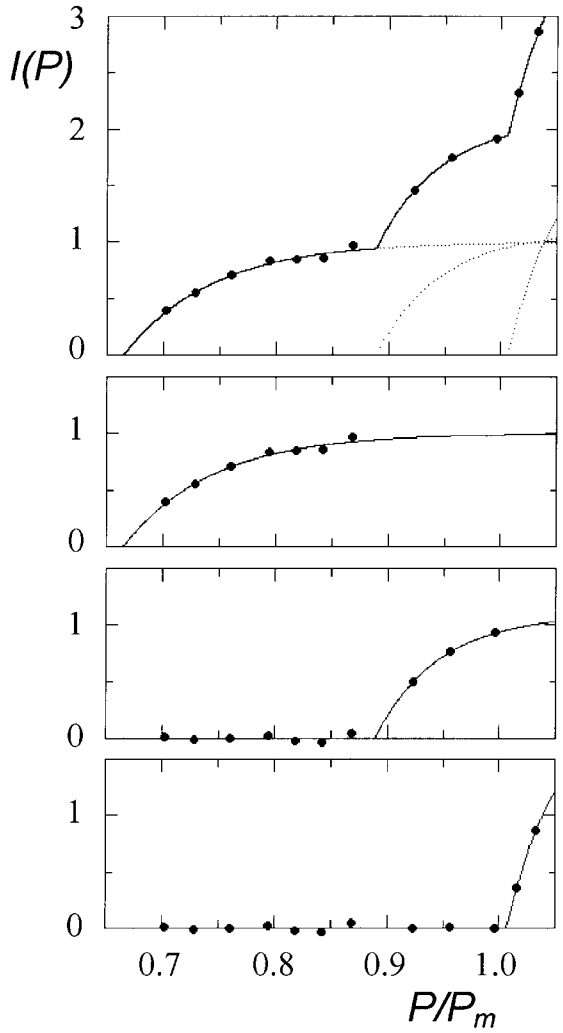

Fig. 12 Vibro-acoustic estimate of cavitation intensity found in a turbine reveals existence of three cavitation mechanisms which can be simply modelled.

Here M is the number of mechanisms, M=3, $I_m(P)$ is the description of the m-th mechanisms, I_m is its relative amplitude in the fully developed stage, P_c^m the related critical power-value, and P_s^m the parameter having the dimension of power, which specifies the speed of rise of the mechanism's intensity. In the case considered, a further regularity has been found: the P_s^m parameters of the three mechanisms are not independent but instead satisfy the relation

$$P_s^m = P_0^2 / P_c^m$$

in which P_0 is a constant. This peculiarity of the process was interpreted as follows: all the three mechanisms have the same physical nature. In Fig. 12, the upper solid-line diagram presents the total effect, and the dots drawn there are measured values. The three lower figures show the models of the mechanisms together with their experimental estimates. These were obtained by subtracting subsequently the models' values from the experimental estimates.

Proposed measurement procedure

The above review of vibro-acoustic technique suggests that reli-

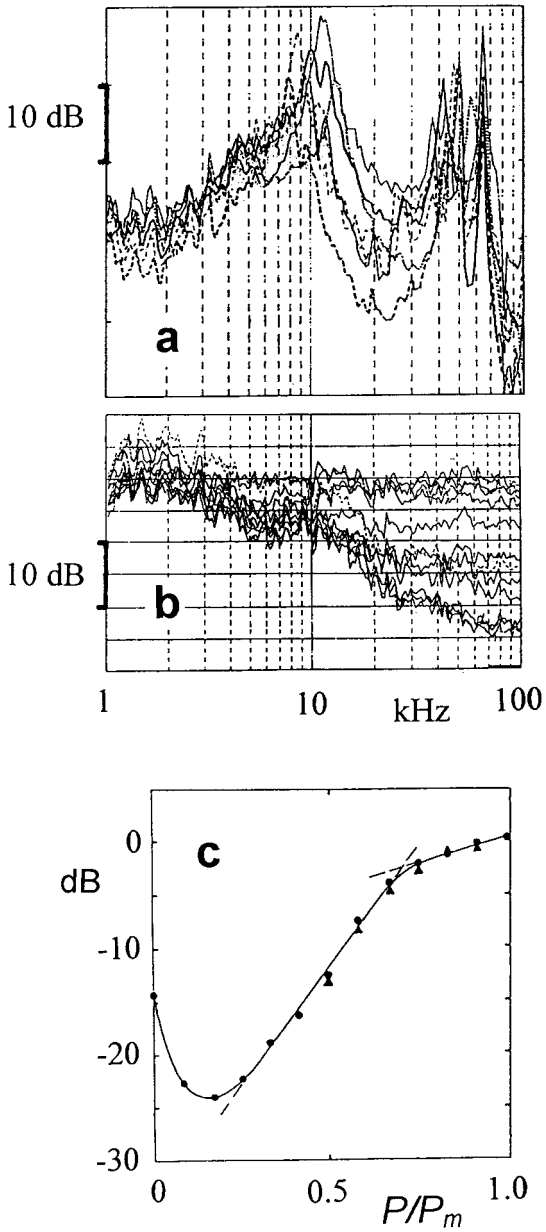

Fig. 13 An example of optimisation of plant operation to minimise cavitation erosion: a – cavitation noise spectra recorded at the same power in different runners (eight of them in four Francis twin-turbines); b – normalised spectra obtained at one of the runners at various power values; c – cavitation characteristics for that runner derived from the normalised spectra (cavitation intensity vs. power, two dot types denote estimates obtained using two types of sensors). The abrupt change of the slope of the cavitation characteristics reveals the threshold of the erosive mechanism. Although nominally identical, the eight runners were very different with respect to cavitation (cf. figure a), and the respective threshold power-values were different. This enabled optimisation of load distribution in seasons with less water, when the full capacity of the plant cannot be used.

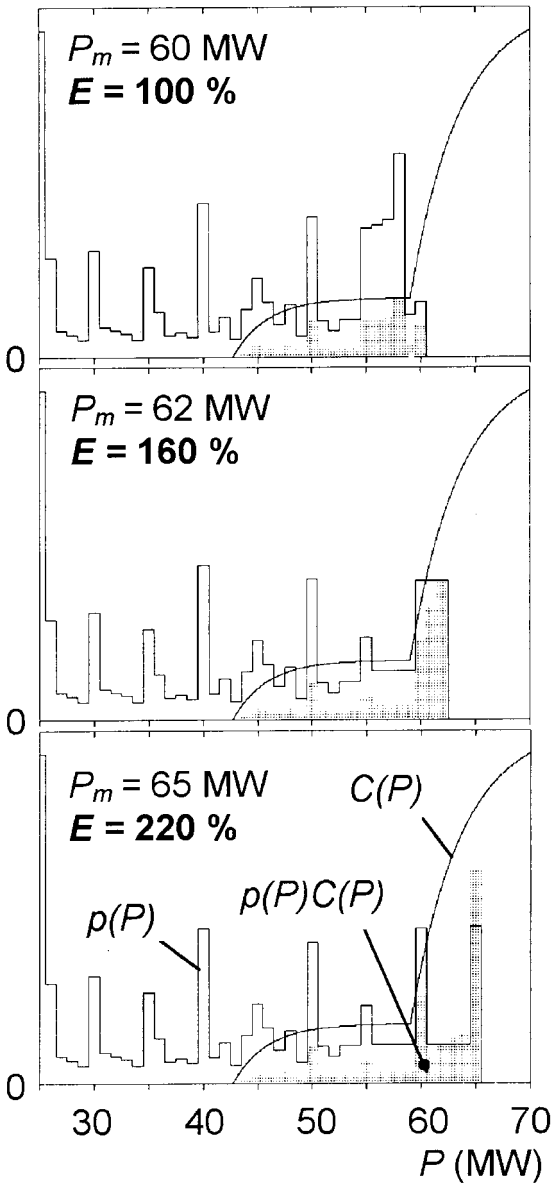

Fig. 14 An example of erosion prediction. A Kaplan turbine rated at the maximum power, P_m, of 60 MW had to be uprated to 62 or 65 MW. The non-calibrated estimate of the cavitation-erosion rate, $C(P)$, derived vibro-acoustically as a function of turbine power P, was combined with the statistics of the actual yearly power-usage, $p(P)$, shown in the upper figure to yield an estimate of the total erosion, $E \sim \int p(P)C(P)dP$, of E=100%. The planned strategies of power-usage after the uprating, shown in the other two figures, yielded then the noted estimates of the total-erosion changes. The two parts of the $C(P)$-curve are found to describe the two mechanisms identified in Fig. 1. The high-power one is the mechanism 2, the origin of which was explained in Fig. 8. Thus, the predicted steep rise of erosion rate can be cured, and practically zero change of erosion can then be expected instead of 160% or 220%, which were predicted for the given state of the turbine.

able and informative diagnosis of turbine cavitation may be obtained by the following actions:

1. Integrate the analysis in four domains – noise frequency, runner's angular position, sensor's position, parameters specifying turbine operational condition. Ensure broad enough coverage of frequency and the other variables.
2. Make the procedure multidimensional, rather than a series of steps restricted to a single domain without resolving in the others.
3. Base the analysis on empirical models to highlight relation-

ships, and construct the models iteratively.
4. Use reliable estimates of background components based on peak-selective spectra.
5. After having identified different cavitation mechanisms, process them separately and combine results into an estimate of the total effect.
6. Proceed similarly for cavitation related to different turbine parts.
7. Quantify a cavitation mechanism or the role of a turbine part by using estimates based on the entire spectra related to them, averaged over a set of representative sensor positions.

Suggestions for plant practice

First make a plant-specific diagnostic test in order to produce a reliable and detailed diagnosis in which cavitation characteristics of a turbine will be assessed and the particularities and peculiarities of the turbine will be revealed and quantified.
Then organise or re-program the monitoring according to these findings. Include within it a suitable form of the inflow decomposition technique in order to make the early detection of detrimental effects and malfunctioning more sensitive and informative.
Run the detailed tests periodically and whenever the monitoring shows anomalies. Such repeated actions should be based on the models developed in previous steps.

Practical end-results

Cavitation characteristics of a turbine which enable identification of operational conditions that are more exposed or less exposed to cavitation. This makes possible the optimisation of the operation with respect to cavitation (Fig. 13).

Selective diagnosis of cavitation mechanisms with respect to turbine parts (guide-vanes, runner blades etc.). This enables identification of weak points with respect to cavitation, suggests potential repairs, and enables confirmation of repair results (cf. Fig. 8 and 14).

Prediction of a change of cavitation characteristics in changed operational conditions (e.g., after uprating, as shown in Fig. 14, or after a change of the relationship of angular positions of guide vanes and runner blades). The prediction is based on data collected in a previous state of the turbine. In some cases a short simulation of new states or operational conditions is necessary.

Algorithm of a selective tailor-made cavitation monitoring system. The system is based on an insight into the particularities and peculiarities of cavitation in a considered turbine and is selective with respect to turbines parts. This guarantees high reliability of the monitoring because the results convey a higher information content and the system's sensitivity is high. This may be crucial in an early detection of detrimental effects (Fig. 15).

Conclusion

The simplest way of making vibro-acoustic diagnosis of turbine cavitation – one sensor location, noise level in a frequency band as an estimator – may yield erroneous results. A systematic study of problems of sampling, processing, analysing, and interpreting

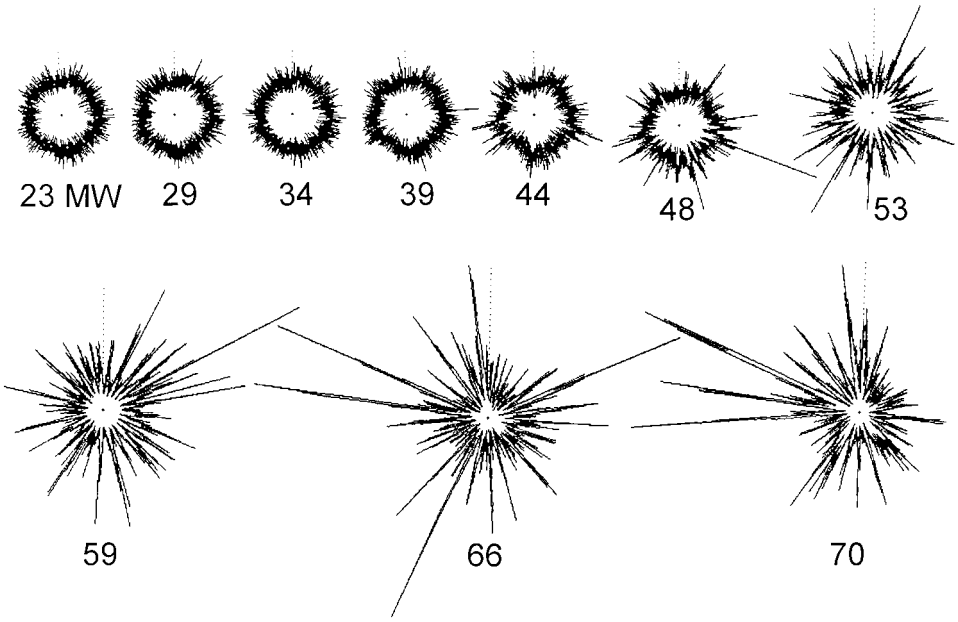

Fig. 15 A pattern of cavitation noise modulation contains data on cavitation details at each turbine power value. Here is an example for a Kaplan turbine. Changes in cavitation that appear in exploitation through the increase of roughness due to abrasion or erosion, or through damages to wetted turbine parts, are reflected as new peaks or changes in existing peaks. Even if these changes may hardly be detected in mean values, they can be readily identified in the curves resolving the runner's position. This increases the sensitivity of monitoring and makes its result more informative.

vibro-acoustic diagnostic data, based on prototype and model experiments, revealed this and some other weak points in the current diagnostic practice. The study resulted in necessary improvements to existing diagnostic procedures and in several new diagnostic techniques. The final results obtainable with the new procedures and techniques range from assessing cavitation which can not be seen in a model test due to inconvenient model form, to early detection of detrimental effects met in turbine exploitation, and to inferences into the details of cavitation mechanisms. The measurement, analysis, and interpretation procedures should be multidimensional, involving noise frequency, runner angular position, sensor position, and variables describing operational conditions of a turbine.

Acknowledgement

The research was done within a project supported by the Turboinstitute, Ljubljana, Slovenia, the German Ministry of Research and Technology, and the Croatian Ministry of Science and Technology.

References

1. Bourdon, P., Simoneau, R., and Avellan, F., 1993, in: Bubble Noise and Cavitation Erosion in Fluid Systems, Proceedings of the ASME Symposium, New Orleans, Louisiana, USA, American Society of Mechanical Engineers, FED-Vol. 176, pp. 51-67.
2. Farhat, M., Bourdon, P., Lavigne, P., and Simoneau, R., 1997, in: Proceedings of the ASME Fluids Engineering Division Summer Meeting, Vancouver, Canada, American Society of Mechanical Engineers, Vol. FEDSM'97.
3. Abbot, P. A., 1989, in: Proceedings of the International Symposium on Cavitation Noise and Erosion in Fluid Systems, San Francisco, California, USA, American Society of Mechanical Engineers, FED-Vol. 88, pp. 55-61.
4. Abbot, P. A., and Morton, D. W., 1991, in: Hydroacoustics Facilities, Instrumentation and Experimental Techniques, Proceedings of the ASME Annual Meeting, Atlanta, Georgia, USA, American Society of Mechanical Engineers, NCA-Vol. 10, pp. 75-84.
5. Gülich, J.-F., 1992, Technische Rundschau Sulzer, No. 1, pp. 30-35.
6. Knapp, W., Schneider, Ch., and Schilling, R., 1992, in: Cavitation, Proceedings of the I Mech E International Conference, Robinson College, Cambridge, C453/048, pp. 271-275.
7. Bajic, B., and Keller, A., 1995, in: Proceedings of the International Symposium on Cavitation CAV'95, Deauville, France, DCN Bassin d'Essais des Carènes, 7-13; also: Transactions of the ASME – Journal of Fluids Engineering, Vol. 118, pp. 756-761.
8. Farhat, M., Bourdon, P., and Lavigne, P., 1996, in: Proceedings of the Conference Modelling, Testing & Monitoring for Hydro Powerplants II, Lausanne, Switzerland, The International Journal on Hydropower & Dams, pp. 151-160.
9. Vizmanos, C., Egusquiza, E., and Jou, E., 1996, in: Proceedings of the Conference Modelling, Testing & Monitoring for Hydro Powerplants II, Lausanne, Switzerland, The International Journal on Hydropower & Dams, pp. 161-168.
10. Bajic, B., 1996, in: Proceedings of the Conference Modelling, Testing & Monitoring for Hydro Powerplants II, Lausanne, Switzerland, The International Journal on Hydropower & Dams, pp. 169-178.
11. Kaye, M., Holenstein, A., Dupont, Ph., and Rettich, J., 1996, in: Proceedings of the Conference Modelling, Testing & Monitoring for Hydro Powerplants II, Lausanne, Switzerland, The International Journal on Hydropower & Dams, pp. 179-188.
12. Bourdon, P., Farhat, M., Simoneau, R., Pereira, F., Dupont, P., Avellan, F., and Dorey, J.-M., 1996, in: Hydraulic Machinery and Cavitation: Proceedings of the XVIII IAHR Symposium on Hydraulic Machinery and Cavitation, Valencia, Spain, Polytechnic University of Valencia, Vol. 1, pp. 534-543.
13. Dorey, J.-M., Laperrousaz, E., Avellan, F., Dupont, P., Simoneau, R., and Bourdon, P., 1996, in: Hydraulic Machinery and Cavitation: Proceedings of the XVIII IAHR Symposium on Hydraulic Machinery and Cavitation, Valencia, Spain, Polytechnic University of Valencia, Vol. 1, pp. 564-573.
14. Dupont, Ph., Caron, J.-F., Avellan, F., Bourdon, P., Lavigne, P., Farhat, M., Simoneau, R., Dorey, J.-M., Archer, A., Laperrousaz, E., and Couston, M., 1996, in: Hydraulic Machinery and Cavitation: Proceedings of the XVIII IAHR Symposium on Hydraulic Machinery and Cavitation, Valencia, Spain, Polytechnic University of Valencia, Vol. 1, pp. 574-583.
15. Bajic, B., 1996, The International Journal on Hydropower & Dams, Vol. 3, pp. 45-50.
16. Bajic, B., 1997, in: Proceedimgs of the Conference Hydropower Into the Next Century, Portoroz, Slovenia, The International Journal on Hydropower & Dams, pp. 185-196.
17. Bajic, B., 1998, Wasserwirtschaft, Vol. 88, pp- 26-31.
18. Bajic, B., 1998, in: Proceedings of the Third International Symposium on Cavitation, Grenoble, France, Vol. 1, pp. 359-362.
19. Bajic, B., 1998, in: Proceedings of the Conference Modelling, Testing & Monitoring for Hydro Powerplants III, Aix-en-Provence, France, The International Journal on Hydropower & Dams, pp. 641-652.
20. Bourdon, P., 1995, Hydro Québec, discussion at the International Symposium on Cavitation CAV'95, Deauville, France, DCN Bassin d'Essais des Carènes.